Lung Bone Marrow–derived Hematopoietic Progenitor Cells Enhance Pulmonary Fibrosis

Taku Nakashima[1], Tianju Liu[1], Hongfeng Yu[1], Lin Ding[1], Matthew Ullenbruch[1], Biao Hu[1], Zhe Wu[1], Hideyuki Oguro[2], and Sem H. Phan[1]

[1]Department of Pathology, University of Michigan Medical School, Ann Arbor, Michigan; and [2]Children's Medical Center Research Institute at UT Southwestern, Dallas, Texas

Rationale: Bone marrow (BM)-derived cells have been implicated in pulmonary fibrosis. However, their precise role in pathogenesis is incompletely understood.

Objectives: To elucidate roles of BM-derived cells in bleomycin-induced pulmonary fibrosis, and clarify their potential relationship to lung hematopoietic progenitor cells (LHPCs).

Methods: GFP BM-chimera mice treated with or without bleomycin were used to assess the BM-derived cells.

Measurements and Main Results: GFP$^+$ cells in the chimera lung were found to be comprised of two distinct phenotypes: GFP^{hi} and GFP^{low} cells. The GFP^{hi}, but not GFP^{low}, population was significantly increased after bleomycin treatment. Flow-cytometric analysis and quantitative real-time polymerase chain reaction revealed that GFP^{hi} cells exhibited phenotypic characteristics of CD11c$^+$ dendritic cells and macrophages. GFP^{hi} cell conditioned media were chemotactic for fibroblasts obtained from fibrotic but not normal lung *in vitro*. Moreover, adoptive transfer of GFP^{hi} cells exacerbated fibrosis in recipient mice, similar to that seen on adoptive transfer of BM-derived CD11c$^+$ cells from donor bleomycin-treated mice. Next, we evaluated the potential of LHPCs as the source of GFP^{hi} cells. Isolation of LHPCs by flow sorting revealed enrichment in cKit$^+$/Sca1$^-$/Lin$^-$ cells, most of which were GFP$^+$ indicating their BM origin. The number of LHPCs increased rapidly after bleomycin treatment. Furthermore, stem cell factor induced LHPC proliferation, whereas granulocyte-macrophage–colony stimulating factor induced differentiation to GFP^{hi} cells.

Conclusions: BM-derived LHPCs with a novel phenotype could differentiate into GFP^{hi} cells, which enhanced pulmonary fibrosis. Targeting this mobilized LHPCs might represent a novel therapeutic approach in chronic fibrotic lung diseases.

Keywords: pulmonary fibrosis; bone marrow transplantation; dendritic cells; hematopoietic stem cells; macrophages

AT A GLANCE COMMENTARY

Scientific Knowledge on the Subject

Bone marrow–derived cells have been implicated in pulmonary fibrosis. However, their precise role in pathogenesis is incompletely understood.

What This Study Adds to the Field

Bone marrow–derived cells in the lung were comprised of two distinct subpopulations in GFP bone marrow chimeric mice: GFP^{hi} and GFP^{low} cells. GFP^{hi} cells mostly expressed CD11c and enhanced pulmonary fibrosis on adoptive transfer. Lung hematopoietic progenitor cells were identified and found to be rapidly increased after bleomycin treatment and could serve as the source of these profibrotic CD11c$^+$ GFP^{hi} cells. Thus, the bone marrow may contribute to pulmonary fibrosis by migration of these progenitor cells to the injured lung where they can proliferate and differentiate into these CD11c$^+$ effector cells.

Chronic fibrotic lung diseases may progress to respiratory failure and end-stage disease, such as in idiopathic pulmonary fibrosis. Despite recent advances in research into pathogenetic mechanisms, some of these including idiopathic pulmonary fibrosis remain without effective therapy to reverse or control the fibrotic response (1). Therefore, advancement of current understanding into the mechanisms underlying chronic fibrotic lung disease remains an emergent issue.

Progenitor cells in the bone marrow (BM) are known to be the source of cells in the peripheral blood, some of which are mobilized into the lung interstitium in response to lung injury. These progenitor cells are usually categorized into nonhematopoietic and hematopoietic elements. Although the nonhematopoietic or mesenchymal stem cells are considered to play important supportive roles for the hematopoietic stem cells (HSCs), recent evidence indicates that they may provide some protection against lung injury when purified and transferred to recipients with said injury (2–6). However, HSC-derived (based on CD45 expression) fibroblast-like cells, such as fibrocytes, are reported to be associated with pulmonary fibrosis (7–9). The precise identity and role of these cells in fibrosis are not fully understood and require further elucidation.

As widely accepted, differentiated hematopoietic cells, such as leukocytes, are derived from HSCs residing in the BM. However, hematopoietic progenitor cells have been reported to exist also in the lung, although their differentiation capacity is much less than HSCs from the BM (10). Colony-forming cells (CFCs) have been identified in healthy lung and rapidly increased in number after lung injury, whereas CFCs in the BM are decreased (11). Furthermore, BM-derived HSCs, equivalent to cKit$^+$/Sca1$^+$/Lineage (Lin)$^-$ cells in BM (also known as KSL) are reported to circulate into multiple peripheral organs including lung (12). These BM-derived HSCs give rise to tissue-resident myeloid cells, although it is unclear if they are identical to the CFCs that can be isolated from lung tissue. Nevertheless, in

conjunction with previous evidence for the importance of BM-derived cells (BMDCs) in fibrosis (13–16), the expansion of the lung CFC population with its concomitant reduction in BM in response to lung injury suggests mobilization of BM-derived HSCs may play a significant role in the subsequent fibrosis, although the identity or identities of the cells recruited to the lung and their roles in fibrosis remain uncertain. Hence, the objective of this study was to characterize the phenotype and role of BMDCs in pulmonary fibrosis using the rodent bleomycin (BLM) model. Some results from this study have been previously reported in the form of an abstract (17).

METHODS

Animals

Female 6- to 8-week-old C57BL/6 wild-type (WT) mice and GFP-transgenic mice on C57BL/6 background were purchased from the Jackson Laboratory (003291; Bar Harbor, ME). Pulmonary fibrosis was induced as before (18–20) by the endotracheal injection of 2.5 U/kg body weight BLM (Blenoxane; Mead Johnson, Plainsboro, NJ). Control mice received sterile saline (SAL) alone. GFP-BM chimeras were generated as before (18, 20). Six weeks after BM transplantation, pulmonary fibrosis was induced by endotracheal BLM injection. Where indicated, 5×10^4 sorted GFP^{hi} cells from lungs of BLM-treated GFP-BM chimera donor mice were transferred by endotracheal injection into WT recipient mice treated with BLM 2 days previously. All study protocols were reviewed and approved by the University Committee on Use and Care of Animals at the University of Michigan.

Flow Cytometry and Cell Sorting

Flow-cytometric analyses of lung cells were performed as before (18, 20). Additional detail is provided in the online supplement.

Cell Migration Assay and Coculture

Cell migration assay was analyzed using a 24-well plate and 8.0-μm Pore Polycarbonate Membrane Insert (Corning Incorporated, Corning, NY) precoated with gelatin solution (Attachment Factor; Life Technologies, Grand Island, NY). Lung fibroblasts (passage 3 isolated from BLM- or SAL-treated mice) were incubated with the fluorescent dye Calcein-AM (BD biosciences, San Diego, CA) for 30 minutes at 37°C in Dulbecco's modified Eagle medium with 0.5% bovine serum albumin. The cells (5×10^5/ml) were then added to the upper chamber. Sorted lung GFP^{hi} or GFP^{low} cells (5×10^4 in 100 μl of the same media) were added to the lower chamber. After incubation for 4 hours at 37°C, the migrated fibroblasts on the undersurface of the membrane insert were measured with a fluorescence plate reader (Gemini EM, Molecular Devices, Sunnyvale, CA) using a 490/515-nm filter set. Sorted lung GFP^{hi} or GFP^{low} cells (5×10^4 cells in Dulbecco's modified Eagle medium with 0.5% bovine serum albumin) were further cocultured for 48 hours with lung fibroblasts (5×10^5 cells) isolated from BLM- or SAL-treated mice. In this experiment, to analyze the effect of factors secreted by GFP$^+$ cells (indirect effect), a 24-well plate and 0.5-μm Pore Polycarbonate Membrane Insert (Corning Incorporated) were used. The fibroblasts were placed at lower chamber and sorted lung GFP$^+$ cells were added to upper chamber.

Purification of RNA, Reverse Transcription, and Real-Time Quantitative Polymerase Chain Reaction

Purification of RNA, reverse transcription and real-time quantitative polymerase chain reaction were performed as previously described (21). Additional detail is provided in the online supplement.

Induction and *In Vivo* Transfer of CD11c$^+$ BMDCs

Dendritic cell skewed CD11c$^+$ BMDCs were induced as before (20), and transferred endotracheally into WT recipient mice. Additional detail is provided in the online supplement.

Cell Culture and Colony-Forming Assay

Where indicated, sorted lung hematopoietic progenitor cells (LHPCs; cKit$^+$/Sca1$^-$/Lin$^-$/Ly6c$^-$/CD11c$^-$/F4/80$^-$) were cultured in dishes precoated with gelatin solution in Dulbecco's modified Eagle medium, or serum-free medium (StemPro-34 SFM; Life Technologies) alone or supplemented with 10% fetal calf serum or various growth factors including basic fibroblast growth factor, platelet-derived growth factor, epidermal growth factor, granulocyte-macrophage–colony stimulating factor (GM-CSF), macrophage colony–stimulating factor, or stem cell factor (SCF) (all from R&D systems, Minneapolis, MN, and 20 ng/ml). For colony-forming assay, MethoCult GF M3434 (STEMCELL Technologies Inc., Vancouver, Canada) supplemented with 20 ng/ml thrombopoietin (Peprotech, Rocky Hill, NJ) was used according to the manufacturer's protocol.

Histologic Analysis

The lungs were inflated and fixed with 4% paraformaldehyde, embedded in paraffin, and cut into 5-μm sections. The sections were stained with hematoxylin and eosin or Masson trichrome stain. Two independent pathologists masked to sample identity evaluated the histopathology and assigned Ashcroft scores to slides in each group of five mice (22).

Hydroxyproline Assay

Lung hydroxyproline content was measured in whole lung homogenates as previously described (19, 20).

Statistical Analysis

Data were shown as mean ± SEM. Differences between groups were analyzed using the Mann-Whitney U test. P value less than 0.05 was considered significant. All analyses were performed using a JMP software package (version 8.0; SAS Institute Inc., Cary, NC).

RESULTS

Characteristics of Lung BMDCs in BLM-induced Pulmonary Fibrosis

To determine the phenotype of BMDCs in pulmonary fibrosis, we created GFP-BM chimera mice by transplanting BM cells isolated from GFP transgenic mice into irradiated WT mice, and after stable engraftment the mice were treated with BLM or SAL. Analysis of the BM-derived GFP$^+$ populations in the lung tissues of control mice and BLM-treated mice revealed two distinct phenotypes: GFP^{hi} with high side scatter and GFP^{low} with low side scatter (Figure 1A). However, the GFP^{hi}, but not GFP^{low}, population was found to be significantly increased (greater than fourfold) in the injured lung after BLM treatment (Figure 1B). In contrast to the lung, analysis of GFP$^+$ cells in the BM revealed only a single population of GFP^{low} cells devoid of the GFP^{hi} with high side scatter population present in the lung (Figure 1A). Among the analyzed cell surface markers, virtually all lung GFP^{hi} cells from both BLM- or SAL-treated mice were positive for CD11c, CD45, major histocompatibility complex (MHC) class II, and F4/80, indicating a phenotype consistent with dendritic cells and macrophages CX (Figure 1C). Smaller percentages of GFP^{hi} cells expressed CD11b (<10%), Sca1 (<40%), cKit (<10%), and Ly6c (<20%) in SAL-treated control mouse lungs, but which were significantly increased in BLM-treated mouse lungs (>30%, >70%, >50%, and >55%, respectively). Most of the GFP^{hi} cells did not express the fibrocytes markers, CD34 (<0.5%) or type I collagen (<8%). Another fibrocyte marker, CXCR4, was significantly up-regulated in GFP$^+$ cells at early time point (*see* Figure E1 in the online supplement). However, virtually no GFP^{hi} cells coexpressed CXCR4 and type I collagen (<0.3%; *see* Figure E1).
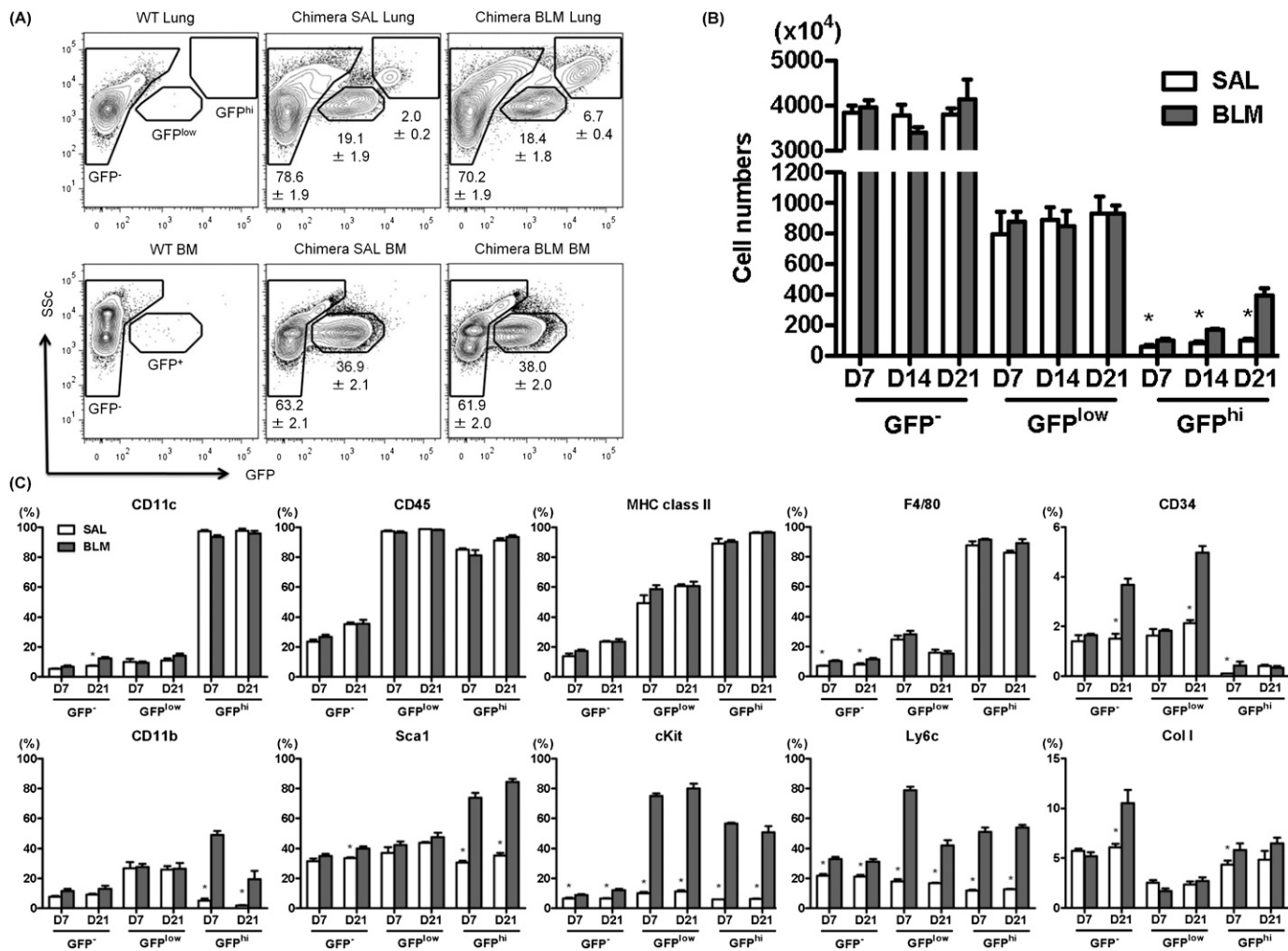
Figure 1. Characteristics of lung bone marrow (BM)-derived cells in bleomycin (BLM)-induced pulmonary fibrosis. (*A*) Single cell suspensions from lung tissue (*top*) or BM (*bottom*) of wild-type (WT) (*left*) nonchimeric mice, control mice (sterile saline [SAL]-treated; *middle*) or BLM-treated (*right*) GFP-BM chimera mice were analyzed by flow cytometry for GFP expression. Analysis of the lung GFP$^+$ populations (n = 6 per group, *top*) revealed two distinct subpopulations of cells with high (GFP^{hi}) or low (GFP^{low}) GFP fluorescence as indicated by the respective gatings. In contrast, in the BM (n = 6 per group, *bottom*), only a single population of GFP^{low} cells was observed. (*B*) Analysis of GFP$^-$, GFP^{low}, and GFP^{hi} cell numbers (n = 3–4 per group) in the GFP-BM chimera lung as a function of time after BLM treatment revealed significant increases above SAL-treated control samples, only in the GFP^{hi} subpopulation at all time points examined. *$P < 0.05$ versus BLM group. (*C*) Flow-cytometric analyses of lung GFP$^-$, GFP^{low}, and GFP^{hi} cells (n = 3–4 per group) after BLM or SAL treatment for the indicated cell markers are shown in the individual panels. *$P < 0.05$ versus BLM group. MHC = major histocompatibility complex.

Although the lung GFP^{low} cells were also virtually all positive for CD45, they have significantly lower proportions of cells expressing CD11c (<20%), MHC class II (<60%), F4/80 (<35%), and type I collagen (<3%). However, relative to the GFP^{hi} cells they have a greater proportion of cells expressing CD34 (>2%), CD11b (>25%), Sca1 (>35%), cKit (>9%), Ly6c (>15%), and CXCR4 (>8%) in the SAL-treated control group, which, except for cKit, CD34 (Day 21 only), Ly6c, and CXCR4 (Day 7 only), were not altered by BLM treatment. The increases in cells expressing cKit and Ly6c were comparable with that seen in the GFP^{hi} cells. Thus, these GFP^{low} cells appeared to be of HSC origin based on CD45 expression, with markers indicative of macrophages and fibrocytes. The BLM-induced increase in cells positive for the stem cell markers Sca1 and cKit in both GFP^{hi} and GFP^{low} populations would be consistent with recruitment and/or proliferation from less-differentiated progenitors in response to injury.

Functional Analysis of Lung BM-derived GFP^{hi} Cells

Next, we sorted the lung GFP$^+$ populations and analyzed their mRNA expression pattern by quantitative real-time polymerase chain reaction. GFP^{hi} cells were obtained by fluorescence-activated cell sorter from GFP-BM chimera mice treated with BLM (BLM-GFP^{hi}) or SAL (SAL-GFP^{hi}). Both sorted BLM-GFP^{hi} (Figure 2A, *left*) and SAL-GFP^{hi} (Figure 2A, *right*) cells attached to the culture plate and showed similar dendritic morphology, but the former appeared larger in size than the latter (n = 5; BLM-GFP^{hi} vs. SAL-GFP^{hi}; 8.6 ± 1.9 vs. 5.7 ± 1.1 μm; $P = 0.02$). BLM-GFP^{hi} and SAL-GFP^{hi} cells expressed a variety of genes associated with inflammation and immune responses (Figure 2B). Among these are genes associated with both M1 (*Ifng*, *Nos2*) and M2 macrophage (*Arg1*, *Fizz1*, *Chi3l3*, and *Igf1*) differentiation. However, only *Arg1* and *Igf1* expression was increased in BLM-GFP^{hi} cells relative to that in SAL-GFP^{hi} cells, whereas *Fizz1* and *Chi3l3* expression was similar in both. In contrast, *Nos2* expression was lower in BLM-GFP^{hi}
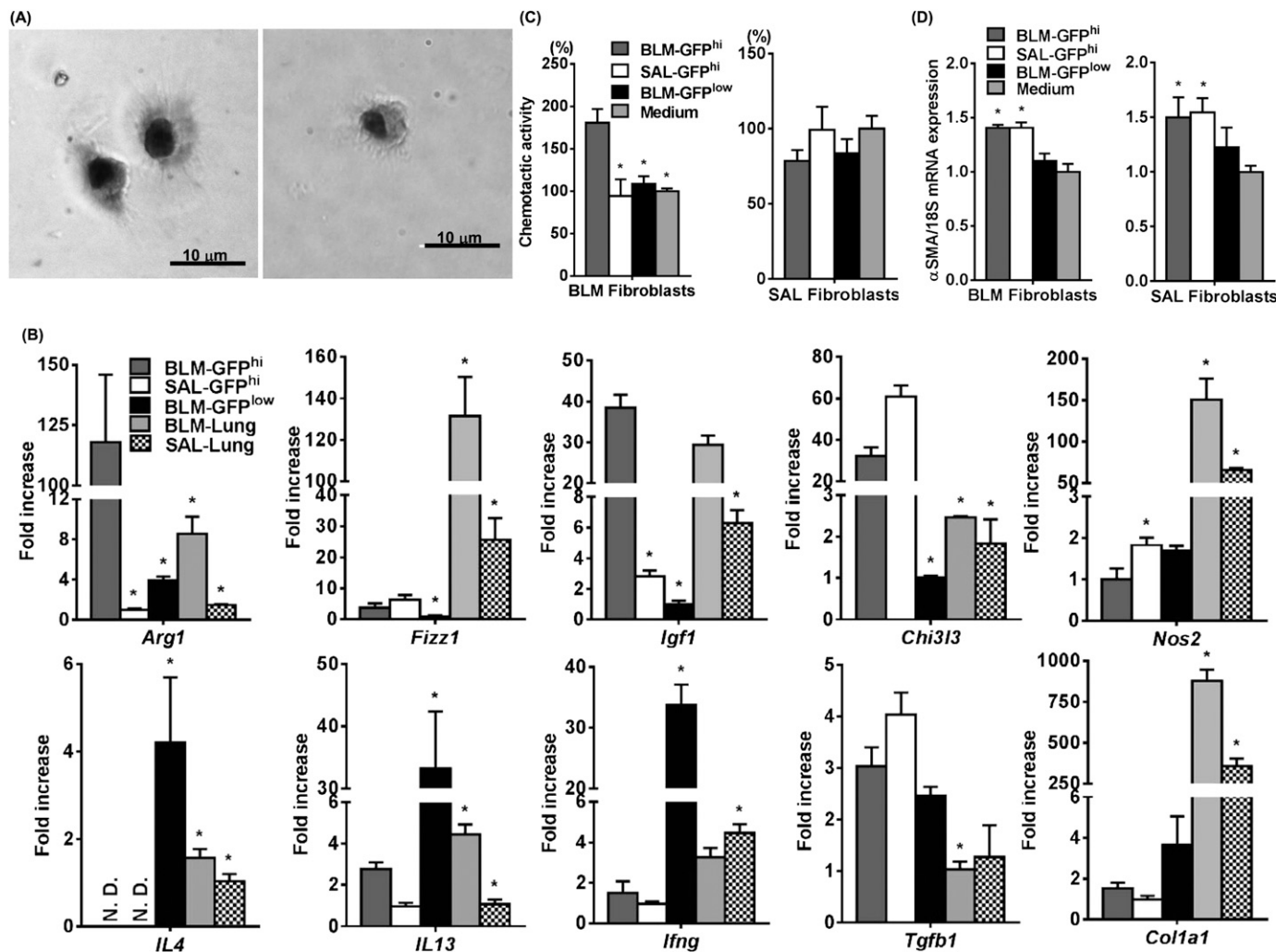
Figure 2. Characteristics of sorted GFP^hi cells. (*A*) Morphology of sorted lung GFP^hi cells, obtained from GFP-BM chimera mice 21 days after treatment with bleomycin (BLM) (BLM-GFP^hi, *left*) or sterile saline (SAL) (SAL-GFP^hi, *right*), under culture is shown by phase-contrast microscopy. Magnification is ×400. (*B*) Expression of the indicated genes, including cytokines, and type I collagen was analyzed by quantitative polymerase chain reaction in BLM-GFP^hi or SAL-GFP^hi, sorted GFP^low cells obtained from GFP-BM chimera mice treated with BLM (BLM-GFP^low), and lung tissues of GFP-BM chimera mice treated with BLM (BLM-Lung) or SAL (SAL-Lung). Measured mRNA levels (n = 3 per group) were expressed relative to internal control *18S* mRNA level and normalized to the lowest value in the each group (which equaled one). *$P < 0.05$ versus BLM-GFP^hi group. (*C*) Chemotactic activity (expressed as % of Medium) of BLM-GFP^hi, SAL-GFP^hi, or BLM-GFP^low cell products (n = 3 per group) for fibroblasts obtained from lungs treated with BLM (BLM Fibroblasts) or SAL (SAL Fibroblasts). *$P < 0.05$ versus BLM-GFP^hi group. (*D*) Effect of BLM-GFP^hi, SAL-GFP^hi, or BLM-GFP^low conditioned media (n = 3–4 per group) on αSMA mRNA expression by fibroblasts obtained from lungs treated with BLM (BLM Fibroblasts) or SAL (SAL Fibroblasts). *$P < 0.05$ versus medium alone.

cells, whereas *Ifng* expression was not significantly different relative to SAL-GFP^hi cells. Although both cell types expressed the Th2 cytokine *IL13*, *IL4* mRNA was not detectable. Both cell types also expressed similar levels of *Tgfb1* and type I collagen (*Col1a1*). However, *Tgfb1* expression in these cells was significantly higher than that in lung tissue, whereas *Col1a1* expression in both GFP^hi and GFP^low cells was much less than in lung tissue. BLM-GFP^low cells primarily exhibited higher levels of both Th1 and Th2 (including *IL4*) cytokine mRNA levels, but lower levels of the other genes relative to those in BLM-GFP^hi cells. Interestingly, when cocultured with murine lung fibroblasts obtained from BLM- or SAL-treated WT mice, only BLM-GFP^hi cells expressed chemotactic activity for fibroblasts from BLM-treated, but not SAL-treated, murine lungs (Figure 2C). Furthermore, when cocultured with murine fibroblasts obtained from BLM- or SAL-treated mice, both BLM-GFP^hi and SAL-GFP^hi cells up-regulated the expression of αSMA mRNA of

the fibroblasts (Figure 2D). Thus, these BMDCs might represent a source of profibrogenic mediators, including the recruitment of fibroblasts and myofibroblast differentiation.

GFP^hi Cells Exacerbated BLM-induced Pulmonary Fibrosis

Given the BLM-induced increased recruitment and altered properties of GFP^hi cells, we next evaluated the role of these cells in BLM-induced pulmonary fibrosis *in vivo*. We isolated BLM-GFP^hi cells by flow sorting and transferred them into recipient WT mice treated with BLM. Endotracheal transfer of BLM-GFP^hi cells into injured lung (2 d after BLM treatment) caused significantly increased lung hydroxyproline content without significant increase in inflammation as measured by recovered cells in the bronchoalveolar lavage fluid (Figures 3A and 3B) when compared with control BLM-treated lung (endotracheally injected with phosphate-buffered saline only
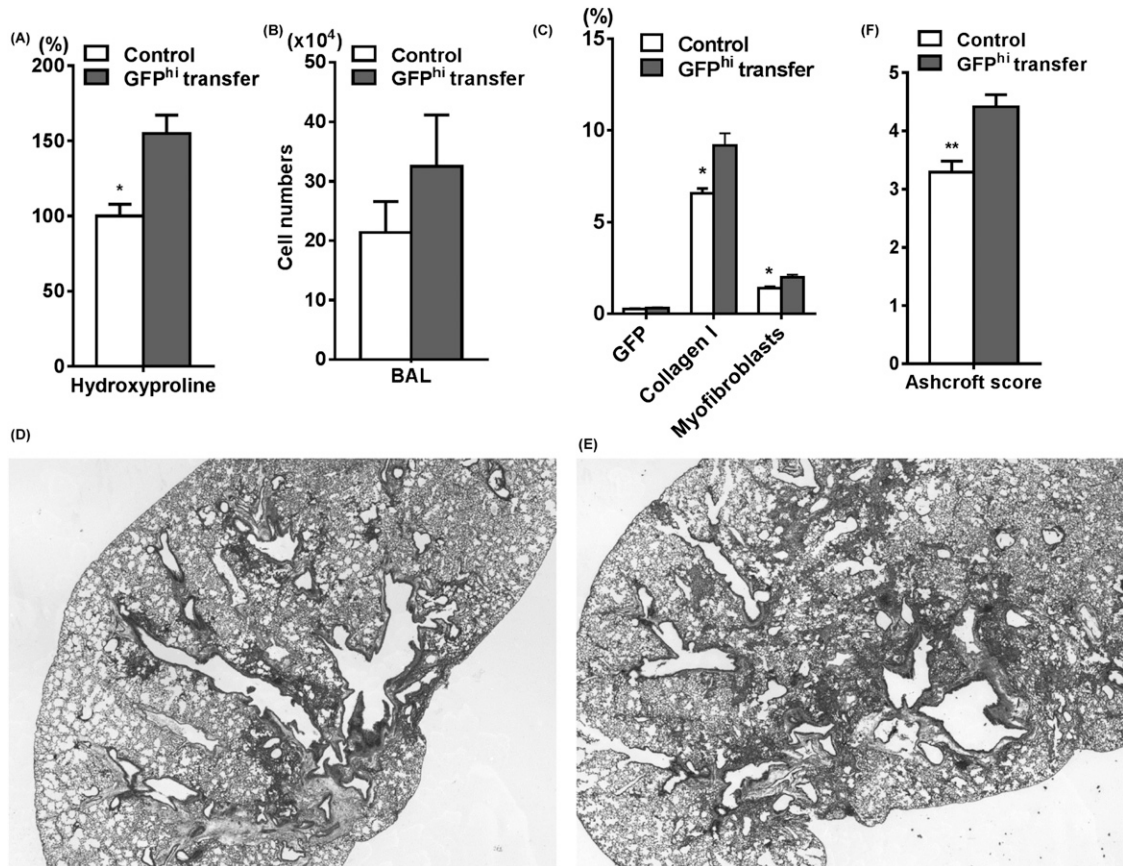
Figure 3. Bleomycin (BLM)-GFP^{hi} cells enhanced BLM-induced pulmonary fibrosis. Sorted BLM-GFP^{hi} cells were transferred endotracheally into recipient wild-type mice, which had been treated with BLM 2 days previously. Control group was transferred phosphate-buffered saline alone. The effects of this cell transfer on (*A*) lung hydroxyproline content (n = 3–4 per group), (*B*) alveolar inflammation (n = 3–8 per group), and (*C*) the percentage of lung cells (n = 4 per group) positive for GFP, collagen I, or myofibroblasts (defined as double positive for collagen I and αSMA) are shown. Masson trichrome–stained lung tissue sections of BLM-treated lung without (*D*) and with BLM-GFP[hi] transfer (*E*) are shown. Magnification is ×40. (*F*) Ashcroft scores were also evaluated as described in the METHODS section using Masson trichrome–stained lung tissue sections of control and BLM-GFP[hi] transfer group. *$P < 0.05$, **$P < 0.01$ versus BLM-GFP[hi] transfer group. BAL = bronchoalveolar lavage.

at 2 d after BLM treatment). This was accompanied by significant increases in collagen I–positive cells and myofibroblasts (double positive cells for collagen I and αSMA) in the lung without increase of GFP^{+} cells (Figure 3C). Compared with control mice (Figure 3D), histologic analysis also confirmed that transfer of BLM-GFP^{hi} cells caused more severe fibrosis (Figure 3E). As shown in Figure 3F, enhanced fibrosis in BLM-GFP[hi] group was also observed on the basis of histopathology evaluated by the Ashcroft score. Thus, endotracheal transfer of a GFP^{hi} subpopulation of BMDCs exacerbated pulmonary fibrosis in this animal model.

Adoptive Transfer of CD11c^{+} BMDCs from BLM-treated Donor Mice Exacerbated BLM-induced Pulmonary Fibrosis

To confirm the profibrotic effect of CD11c^{+} cells derived from BLM-injured mice, and to exclude the possibility of nonspecific effects of increased cell numbers on pulmonary fibrosis, we further evaluated the effect of BMDCs generated from BLM- or SAL-treated mice on pulmonary fibrosis. Induced dendritic cell skewed CD11c^{+} BLM- or SAL-BMDCs were endotracheally transferred into recipient WT mice (3 d after BLM treatment). BLM-BMDCs, but not SAL-BMDCs significantly enhanced lung hydroxyproline content (*see* Figure E2A), which was accompanied by up-regulated type I collagen mRNA expression in the lung (*see* Figure E2B). Thus, enhancement of pulmonary

fibrosis by BMDCs was observed specifically when such cells originated from BLM-injured mice.

Characteristics of HPCs in the Lung

To further elucidate the identity of GFP^{hi} cells, we first analyzed and defined the HPCs in the BM and lung. After BLM treatment, the HPC population changed in the BM with rapid increase in myeloid progenitors, followed by increase in lymphoid progenitors (*see* Figure E3). The number of CFCs in the lung was much smaller relative to the BM and was significantly enriched in Lin[−]/cKit^{+} cells (Figure 4A). However, in contrast to the Lin[−]/cKit^{+} cells in the BM, most of the Lin[−]/cKit^{+} cells in the lung were Sca1^{+} (Figure 4B). We also found that almost 60% of the cKit^{+} cells were both Sca1^{+}/Ly6c^{+} (Figure 4C). Next, to determine the characteristics of HPCs in the lung, we analyzed the colony-forming ability of cKit^{+} populations. The results indicated that cKit^{+}/Ly6c^{+} cells, cKit^{+}/CD11c^{+} cells, and cKit^{+}/F4/80^{+} cells lacked the ability to form colonies (data not shown). After the removal of Ly6c^{+}, CD11c^{+}, and F4/80^{+} cells, the residual fraction of cKit^{+} cells in the lung (cKit^{+} in Lin^{−}/Ly6c^{−}/CD11c^{−}/F4/80^{−}) was very small (Figure 4B). Among this residual (Lin^{−}/Ly6c^{−}/CD11c^{−}/F4/80^{−}) population, only cKit^{+}/Sca1^{−} cells, but not cKit^{+}/Sca1^{+} or cKit^{−}/Sca1^{+} cells, exhibited the enriched colony-forming ability (Figure 4D). These findings suggested that this cKit^{+}/Sca1^{−}/Lin^{−}/Ly6c^{−}/CD11c^{−}/F4/80^{−}
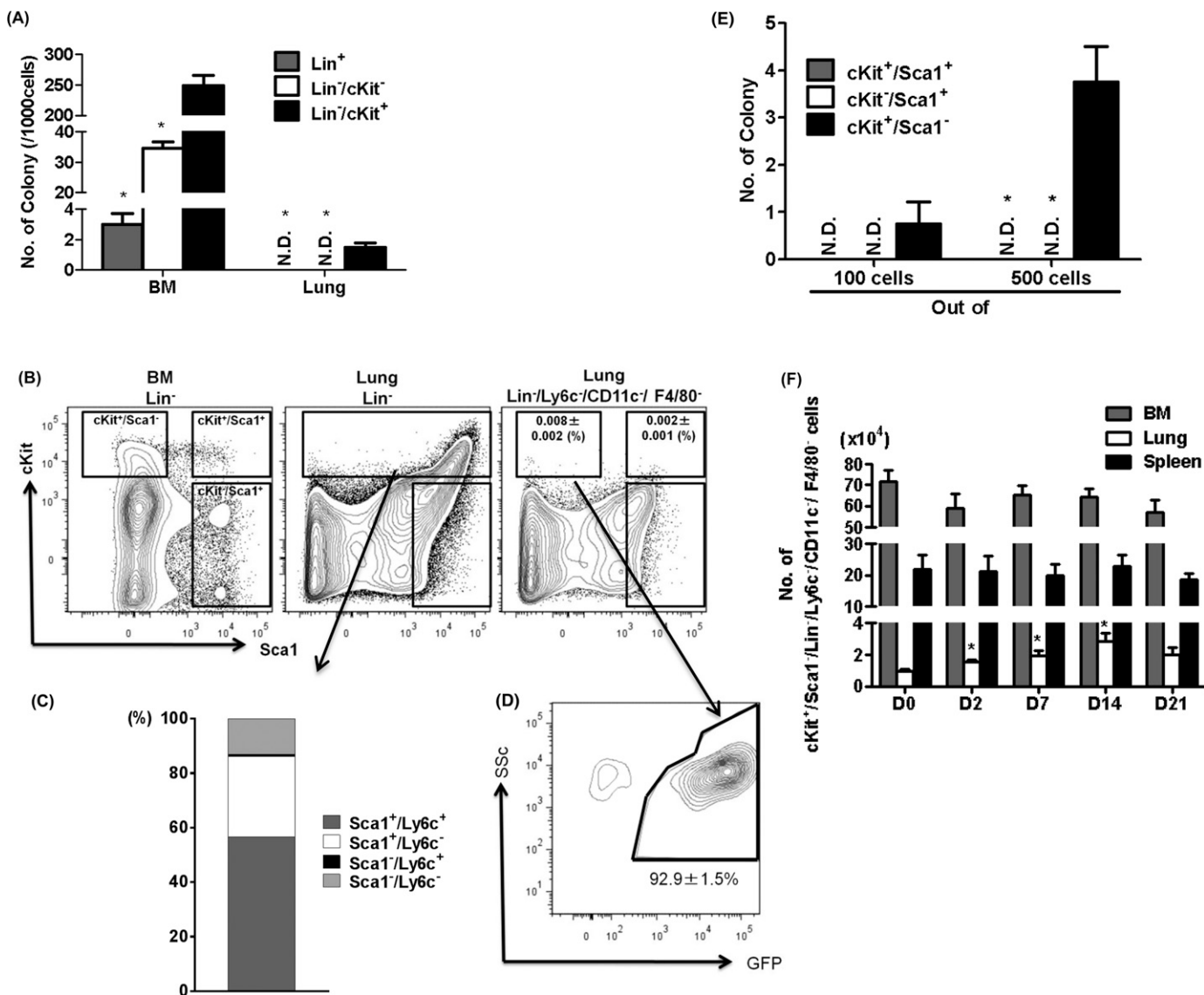
Figure 4. Characteristics of colony-forming cells in the lung. (*A*) Using Methocult colony forming assay, numbers of colony derived from Lin$^+$, Lin$^-$/cKit$^-$, or Lin$^-$/cKit$^+$ cells in the bone marrow (BM) and lung were counted (n = 4 per group). *$P < 0.05$ versus Lin$^-$/cKit$^+$. (*B*) Flow-cytometric analyses of Sca1 and cKit expression in BM Lin$^-$ cells, lung Lin$^-$ cells, or lung Lin$^-$/Ly6c$^-$/CD11c$^-$/F4/80$^-$ cells are shown. The numbers of cKit$^+$/Sca1$^-$/Lin$^-$/Ly6c$^-$/CD11c$^-$/F4/80$^-$ and cKit$^+$/Sca1$^+$/Lin$^-$/Ly6c$^-$/CD11c$^-$/F4/80$^-$ cells in lung were enumerated and shown as percent of total lung cells (n = 4 per group). (*C*) The numbers of Sca1 and Ly6c positivity in lung Lin$^-$/cKit$^+$ cells were enumerated and shown as percent of total. (*D*) Numbers of colonies derived from sorted cKit$^+$/Sca1$^+$, cKit$^-$/Sca1$^+$, or cKit$^+$/Sca1$^-$ cells among the lung Lin$^-$/Ly6c$^-$/CD11c$^-$/F4/80$^-$ cells are shown. *$P < 0.05$ versus cKit$^+$/Sca1$^-$. (*E*) GFP positivity rate in lung cKit$^+$/Sca1$^-$/Lin$^-$/Ly6c$^-$/CD11c$^-$/F4/80$^-$ cells obtained from BM-chimera mice are shown (n = 4 per group). (*F*) Kinetics of cKit$^+$/Sca1$^-$/Lin$^-$/Ly6c$^-$/CD11c$^-$/F4/80$^-$ cells in the BM, lung, and spleen revealed significant increases occurred only in the lung in the BLM-treated mice (n = 3–5 per group). *$P < 0.05$ versus D0.

population comprised the LHPCs. In the GFP-BM chimera mice, more than 90% of LHPCs are GFP$^+$, suggesting that virtually all LHPCs are BM-derived (Figure 4E). After BLM treatment, the LHPC population was significantly increased (greater than three-fold at its peak on Day 14 after BLM treatment) but remained unchanged in the BM or spleen (Figure 4F). This BLM-induced increase in the LHPC population presumably was caused by increased recruitment from the BM and/or proliferation after reaching the lung.

LHPCs as the Source of GFP^{hi}

To evaluate this possibility, LHPCs were purified by flow sorting (using the markers identified previously) from lungs of GFP-BM chimera mice and their differentiation ability assessed *in vitro.*

Sorted LHPCs were cultured in medium with or without serum, and serum-free medium with various growth factors including basic fibroblast growth factor, platelet-derived growth factor, epidermal growth factor, GM-CSF, macrophage colony–stimulating factor, or SCF. The results showed that LHPCs proliferated best in the presence of SCF, although GM-CSF had a weak effect (Figure 5). When cultured in the presence of SCF, LHPCs grew well, forming colonies and differentiating into cells with diverse size and GFP fluorescence intensity (Figures 5C–5F). When cytospun onto slides, most of the differentiated cells in SCF-containing media exhibited mononuclear morphology, whereas some cells showed granular cytoplasm or lobulated nuclei (*see* Figure E4). Analysis by flow cytometry revealed that culturing in the presence of GM-CSF and/or SCF caused these LHPCs to brighten with respect to GFP fluorescence and
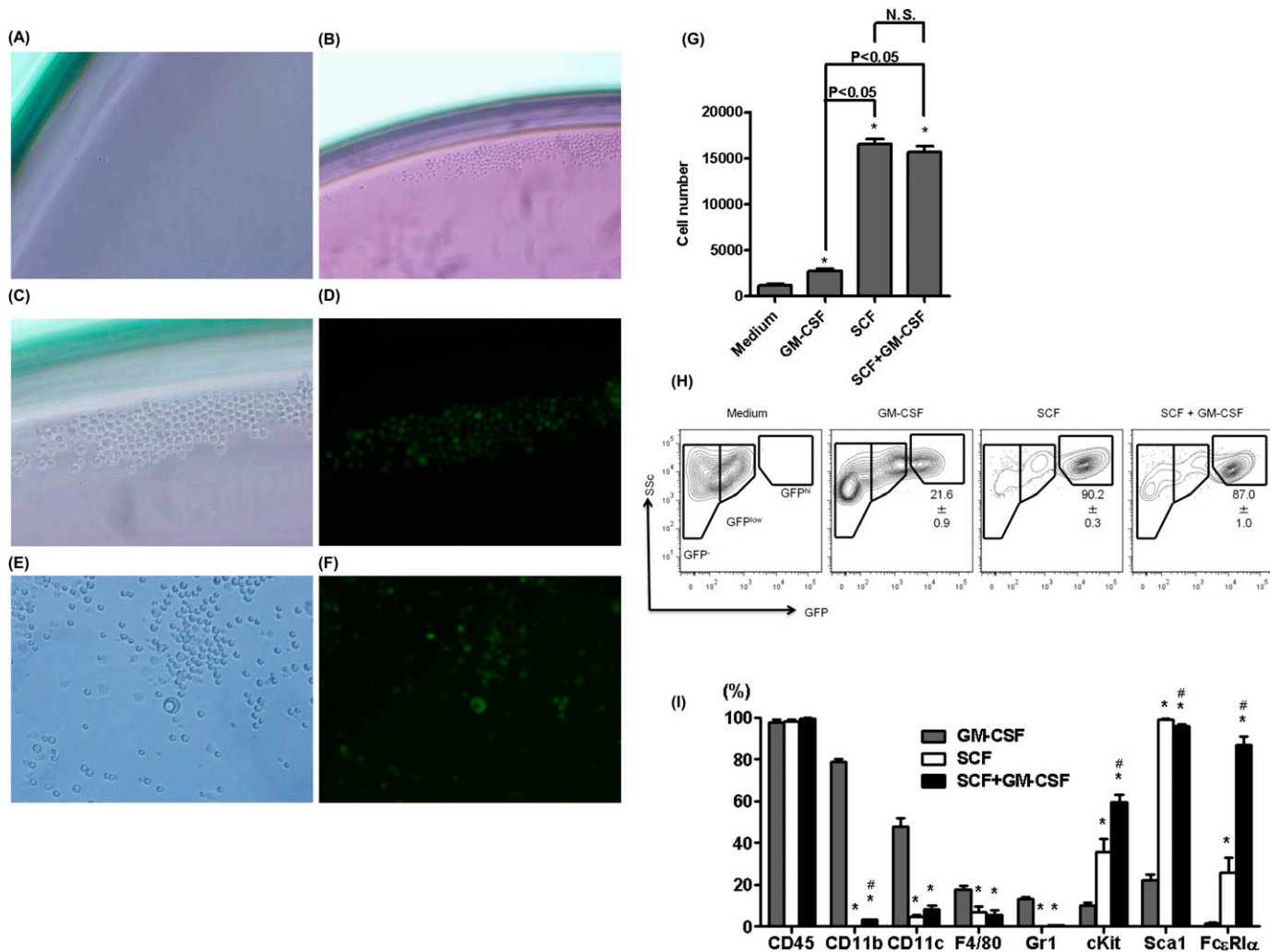
Figure 5. Differentiation ability of sorted bone marrow (BM)-derived hematopoietic progenitor cells (HPCs) in the lung. Directly sorted BM-derived HPCs in the lung (GFP$^+$/cKit$^+$/Sca1$^-$/Lin$^-$/ Ly6c$^-$/CD11c$^-$/ F4/80$^-$ cells) from BM GFP-chimera mice were cultured in media supplemented with serum (A) or stem cell factor (SCF) (B–F). Bright-field (A and B, ×100 magnification; C and E, ×200) and fluorescence (D and F, ×200) micrographs of these cells are shown. (G) Cell numbers of sorted HPCs cultured for 5 days in serum-free media supplemented with or without the indicated growth factors are shown (n = 3 per group). *$P < 0.05$ versus Media alone. (H) Flow-cytometric analyses of cultured HPCs with or without the indicated growth factors (n = 4 per group) are shown to monitor the effect on GFP expression. (I) Flow-cytometric analyses of GFP$^+$ population in growth factor treated cultured HPCs for select cell markers are shown (n = 3 per group). *$P < 0.05$ versus granulocyte-macrophage–colony stimulating factor (GM-SCF) group, #$P < 0.05$ SCF group.

resembled the GFP^{hi} cells with high side scatter present in the lungs of SAL- and BLM-treated mice (Figure 5H). Among the GFP$^+$ population, virtually all the cells expressed CD45 on their cell surface (Figure 5I). GM-CSF induced the expression of CD11b, CD11c, and F4/80 to differing extents, whereas, SCF predominantly induced cKit, Sca1, or FcεRIα expression (Figure 5I). This differentiated pattern of cell surface markers resembled those in the BLM-GFP^{hi} cells (Figure 1C).

DISCUSSION

The current study demonstrated that only a subpopulation of lung BMDCs was increased in BLM-induced pulmonary fibrosis. This subpopulation was characterized by high GFP expression with high side scatter characteristics (GFP^{hi} cells), whereas the GFP^{low} subpopulation was essentially unchanged. Moreover, GFP^{hi} cells were not present in the BM, suggesting that the lung microenvironment was necessary for assumption of the GFP^{hi} phenotype either because of increase in cell size

(consistent with higher side scatter) and/or GFP expression. These GFP^{hi} cells were CD45$^+$ and resembled dendritic cells and macrophages on the basis of marker protein expression (CD11c, MHC class II, and F4/80) and expressed immunoregulatory genes, such as *Tgfb1*, and those associated with both M1 and M2 macrophage differentiation. They resembled fibrocytes by their expression of type I collagen and CD45, but were essentially negative for CD34. Some GFP^{hi} cells were positive for CXCR4, but virtually no GFP^{hi} cells coexpressed both CXCR4 and type I collagen, suggesting that GFP^{hi} subpopulation was essentially devoid of fibrocytes, which coexpress these markers. GFP^{hi} cells obtained from BLM-treated mice exhibited a greater proportion of cells positive for Sca1 and cKit, suggesting an increase in less-differentiated cells. However, increases in the proportion of cells that are positive for CD11b along with the increased expression of *Arg1* and *Igf1* but decreased *Nos2* expression suggested possible differentiation toward an M2 macrophage phenotype, albeit an atypical one given the lack of change in *Fizz1* and *Chi3l3* expression. Nevertheless, the

selective expansion of this lung GFP^{hi} population and its altered composition in BLM-treated mice suggested a significant role for these BMDCs in pulmonary fibrosis. Indeed, these cells were found to secrete chemotactic activity for fibroblast cultures isolated from BLM-injured lungs only since it was inactive for cultures from control SAL-treated lungs. Furthermore, these GFP^{hi} cell conditioned media enhanced myofibroblast differentiation in lung fibroblast cultures. Thus, it is conceivable that these BM-derived GFP^{hi} subpopulations could play a significant role in pulmonary fibrosis by secretion of factors capable of fibroblast recruitment and myofibroblast differentiation that may be critical for expansion of the mesenchymal response and perhaps formation of fibrotic foci. Additionally, the increased expression of *Igf1* by these cells could also promote fibroblast proliferation.

This possible *in vivo* role of the BLM-GFP^{hi} cells was then investigated by examining the effect of transferring these cells on BLM-induced fibrosis in recipient mice. In mice receiving endotracheal transfer of BLM-GFP^{hi} cells there was a significant increase (>50%) in lung hydroxyproline with morphologic evidence of enhanced pulmonary fibrosis relative to control BLM-treated mice. However, this was not accompanied by a significant increase in recovered cells from the bronchoalveolar lavage fluid. Thus, the transfer of these cells by endotracheal instillation caused significant increase in severity of pulmonary fibrosis in recipient mice with BLM-induced lung injury without significant increase in inflammatory cell recruitment. Their ability to recruit fibroblasts and to induce myofibroblasts differentiation as shown *in vivo* and *in vitro* may be a mechanism by which these cells could promote fibrosis, although additional or alternative mechanisms cannot be ruled out at this time.

Phenotypic characterization of the BLM-GFP^{hi} cells revealed most to express markers of progenitor cells, namely cKit and Sca1. In contrast, only a minority of the SAL-GFP^{hi} cells expressed these markers, especially for cKit wherein less than 10% were positive for this marker. This would indicate an expansion in this less mature subpopulation as a consequence of BLM-induced lung injury, either through increased mobilization and recruitment from the BM and/or expansion of progenitors on recruitment to the lung. Similarly, BMDCs, obtained from BLM-treated but not SAL-treated mice, demonstrated exacerbation of pulmonary fibrosis when transferred *in vivo*. Examination of LHPCs (cKit$^+$/Sca1$^-$/Lin$^-$/Ly6c$^-$/CD11c$^-$/F4/80$^-$) revealed them to be derived from the BM and mobilized rapidly at the initiation of pulmonary fibrosis. A recent report suggested that HPCs, which are equivalent to KSL cells, patrol by blood circulation into peripheral organ including lung (12). Surprisingly, CFCs in the lung were highly enriched in cKit$^+$/Sca1$^-$/Lin$^-$, but not KSL population. This population is dissimilar to previously reported lung side population cells, most of which did not express cKit (10). The BM-derived HPCs in the current study, namely LHPCs, can differentiate into CD11b$^+$/CD11c$^+$/GFP^{hi} cells that are predominantly cKit negative when cultured with GM-CSF. However, SCF, the ligand for cKit, significantly increased LHPC proliferation with promotion of cKit and Sca1 expression. Because granulocyte and monocyte progenitors give rise to monocytes-macrophages and mast cells (23), LHPCs may be equivalent to myeloid progenitors including common myeloid progenitors, and granulocyte-monocyte progenitors. This notion is consistent with the noted increase in BM myeloid progenitors immediately after BLM treatment. The potential of LHPCs as a source of the profibrotic BLM-GFP^{hi} cells is also supported by the ability of GM-CSF and/or SCF to induce appearance of these cells *in vitro*. This could represent a possible explanation for the appearance of these cells only on mobilization to the lung. Indeed, SCF is significantly up-regulated in the BLM-injured lung, and increases the number of BMDCs mobilized to the lung (24).

To date, several lines of evidences suggested that BMDCs, including fibrocytes, expressed collagen (7, 18, 25, 26). Although collagen-expressing BMDCs likely exist, their definition as fibrocytes is not straightforward because of the lack of stable unique markers for this cell type, with many of the markers used being also expressed by any number of different cell types, including macrophages and dendritic cells (8, 27). Our results showed that virtually all of the BM-derived GFP$^+$ cells were CD45$^+$ with a small proportion (<10%) being type I collagen–positive. Moreover, the GFP^{hi} cells were mostly (>99%) negative for CD34, lack coexpression of CXCR4/type I collagen, and did not exhibit spindle-shaped morphology, all of which are widely accepted characteristics of fibrocytes. Thus, we conclude that GFP^{hi} cells did not fit the definition of fibrocytes, which would be consistent with a recent report by Barisic-Dujmovic and coworkers (25).

Thus, the precise identity of these BLM-GFP^{hi} cells remains uncertain. They expressed some markers (*Arg1*, *Chi3l3*) that characterize alternatively activated or M2 macrophages, which are known to be increased in rodent and human fibrotic lung (28, 29). Furthermore, the depletion of macrophages by clodronate resulted in reduced pulmonary fibrosis (28). Macrophages are generally considered as monocyte-derived cells, and using transfer of donor-derived Ly6c^{hi} monocytes, Gibbons and coworkers (28) cannot find any donor-derived M2 macrophages in the recipient. Our results also demonstrated that GFP^{hi} cells (more than half of them were Ly6c$^+$) did not expand when transferred *in vivo* (Figure 3C). Taken together, these findings suggest that Ly6c$^+$ cells are more differentiated cells and the origin of M2 macrophages seem to exist in the Ly6c$^-$ population, as recently reviewed (30). Despite this M2 marker expression, the GFP^{hi} cells also express M1 macrophage markers (*Nos2*, *Ifng*) and expression of the M2 marker, *Fizz1*, was quite low and actually reduced in BLM-GFP^{hi} cells relative to that in SAL-GFP^{hi} cells, indicating an atypical M1 versus M2 differentiation pattern. Another complicating factor is that virtually all these cells expressed CD11c, whereas only a minority expressed CD11b. To distinguish alveolar macrophages from dendritic cells, F4/80 expression on cell surface is often used together with CD11c (31). However, F4/80 is also expressed by some dendritic cells, especially those that are less mature (32). Thus, cell surface markers alone do not clearly define cellular identity (32, 33), and it may be prudent to consider these GFP^{hi} cells as dendritic cells and macrophages. The importance of dendritic cells in BLM-induced pulmonary fibrosis has been demonstrated, and increased numbers of these cells have been reported in lungs of patients with fibrotic interstitial lung disease, including idiopathic pulmonary fibrosis (34, 35). However, the presence of LHPCs in human lung remains to be demonstrated and because of ethical considerations their origin and fate cannot be tracked by transgenic GFP expression. Thus, there remains some uncertainty with respect to the identity of the human counterpart of the murine GFP^{hi} cells and their progenitors, and their relevance to human lung biology and disease.

In conclusion, the current study showed the recruitment of BM-derived progenitor cells to the lung in pulmonary fibrosis, which on mobilization to the lung gave rise to a distinct subpopulation exhibiting markers consistent with dendritic cells and macrophages. This subpopulation enhanced fibrosis when transferred to recipient mice with lung injury, and was shown to secrete fibroblast chemoattractant activity *in vitro*. The findings taken together indicate that the recruited cells from the BM represent less mature progenitor cells, which differentiate on reaching the lung to the dendritic cell and macrophage-like

phenotype and subsequently contribute to fibrogenesis in a para-
crine manner.

References

1. Noble PW, Barkauskas CE, Jiang D. Pulmonary fibrosis: patterns and perpetrators. *J Clin Invest* 2012;122:2756–2762.
2. Gupta N, Su X, Popov B, Lee JW, Serikov V, Matthay MA. Intrapulmonary delivery of bone marrow-derived mesenchymal stem cells improves survival and attenuates endotoxin-induced acute lung injury in mice. *J Immunol* 2007;179:1855–1863.
3. Rojas M, Xu J, Woods CR, Mora AL, Spears W, Roman J, Brigham KL. Bone marrow-derived mesenchymal stem cells in repair of the injured lung. *Am J Respir Cell Mol Biol* 2005;33:145–152.
4. Lee JW, Fang X, Krasnodembskaya A, Howard JP, Matthay MA. Concise review: mesenchymal stem cells for acute lung injury: role of paracrine soluble factors. *Stem Cells* 2011;29:913–919.
5. Ortiz LA, Dutreil M, Fattman C, Pandey AC, Torres G, Go K, Phinney DG. Interleukin 1 receptor antagonist mediates the antiinflammatory and antifibrotic effect of mesenchymal stem cells during lung injury. *Proc Natl Acad Sci USA* 2007;104:11002–11007.
6. Kassmer SH, Bruscia EM, Zhang PX, Krause DS. Nonhematopoietic cells are the primary source of bone marrow-derived lung epithelial cells. *Stem Cells* 2012;30:491–499.
7. Phan SH. Genesis of the myofibroblast in lung injury and fibrosis. *Proc Am Thorac Soc* 2012;9:148–152.
8. Reilkoff RA, Bucala R, Herzog EL. Fibrocytes: emerging effector cells in chronic inflammation. *Nat Rev Immunol* 2011;11:427–435.
9. Moeller A, Gilpin SE, Ask K, Cox G, Cook D, Gauldie J, Margetts PJ, Farkas L, Dobranowski J, Boylan C, et al. Circulating fibrocytes are an indicator of poor prognosis in idiopathic pulmonary fibrosis. *Am J Respir Crit Care Med* 2009;179:588–594.
10. Abe S, Lauby G, Boyer C, Manouilova L, Rennard SI, Sharp JG. Lung cells transplanted to irradiated recipients generate lymphohematopoietic progeny. *Am J Respir Cell Mol Biol* 2004;30:491–499.
11. Badami CD, Livingston DH, Sifri ZC, Caputo FJ, Bonilla L, Mohr AM, Deitch EA. Hematopoietic progenitor cells mobilize to the site of injury after trauma and hemorrhagic shock in rats. *J Trauma* 2007;63:596–600; discussion 600–592.
12. Massberg S, Schaerli P, Knezevic-Maramica I, Köllnberger M, Tubo N, Moseman EA, Huff IV, Junt T, Wagers AJ, Mazo IB, et al. Immunosurveillance by hematopoietic progenitor cells trafficking through blood, lymph, and peripheral tissues. *Cell* 2007;131:994–1008.
13. Aono Y, Ledford JG, Mukherjee S, Ogawa H, Nishioka Y, Sone S, Beers MF, Noble PW, Wright JR. Surfactant protein-D regulates effector cell function and fibrotic lung remodeling in response to bleomycin injury. *Am J Respir Crit Care Med* 2012;185:525–536.
14. Murray LA, Chen Q, Kramer MS, Hesson DP, Argentieri RL, Peng X, Gulati M, Homer RJ, Russell T, van Rooijen N, et al. TGF-beta driven lung fibrosis is macrophage dependent and blocked by Serum amyloid P. *Int J Biochem Cell Biol* 2011;43:154–162.
15. Tourkina E, Bonner M, Oates J, Hofbauer A, Richard M, Znoyko S, Visconti RP, Zhang J, Hatfield CM, Silver RM, et al. Altered monocyte and fibrocyte phenotype and function in scleroderma interstitial lung disease: reversal by caveolin-1 scaffolding domain peptide. *Fibrogenesis Tissue Repair* 2011;4:15.
16. Vannella KM, Luckhardt TR, Wilke CA, van Dyk LF, Toews GB, Moore BB. Latent herpesvirus infection augments experimental pulmonary fibrosis. *Am J Respir Crit Care Med* 2010;181:465–477.
17. Nakashima T, Ding L, Yu H, Liu J, Wu Z, Ullenbruch M, Hu B, Liu T, Phan SH. Bone marrow-derived cells accelerate bleomycin induced pulmonary fibrosis in mice [abstract]. *Am J Respir Crit Care Med* 2012;185:A6243.
18. Hashimoto N, Jin H, Liu T, Chensue SW, Phan SH. Bone marrow-derived progenitor cells in pulmonary fibrosis. *J Clin Invest* 2004; 113:243–252.
19. Hu B, Wu Z, Nakashima T, Phan SH. Mesenchymal-specific deletion of C/EBPβ suppresses pulmonary fibrosis. *Am J Pathol* 2012;180:2257–2267.
20. Liu T, Baek HA, Yu H, Lee HJ, Park BH, Ullenbruch M, Liu J, Nakashima T, Choi YY, Wu GD, et al. FIZZ2/RELM-β induction and role in pulmonary fibrosis. *J Immunol* 2011;187:450–461.
21. Nakashima T, Yokoyama A, Onari Y, Shoda H, Haruta Y, Hattori N, Naka T, Kohno N. Suppressor of cytokine signaling 1 inhibits pulmonary inflammation and fibrosis. *J Allergy Clin Immunol* 2008;121:1269–1276.
22. Ashcroft T, Simpson JM, Timbrell V. Simple method of estimating severity of pulmonary fibrosis on a numerical scale. *J Clin Pathol* 1988;41:467–470.
23. Arinobu Y, Iwasaki H, Akashi K. Origin of basophils and mast cells. *Allergol Int* 2009;58:21–28.
24. Ding L, Dolgachev V, Wu Z, Liu T, Nakashima T, Wu Z, Ullenbruch M, Lukacs NW, Chen Z, Phan SH. Essential role of stem cell factor-c-Kit signalling pathway in bleomycin-induced pulmonary fibrosis. *J Pathol* 2013;230:205–214.
25. Barisic-Dujmovic T, Boban I, Clark SH. Fibroblasts/myofibroblasts that participate in cutaneous wound healing are not derived from circulating progenitor cells. *J Cell Physiol* 2010;222:703–712.
26. Opalenik SR, Davidson JM. Fibroblast differentiation of bone marrow-derived cells during wound repair. *FASEB J* 2005;19:1561–1563.
27. Pilling D, Fan T, Huang D, Kaul B, Gomer RH. Identification of markers that distinguish monocyte-derived fibrocytes from monocytes, macrophages, and fibroblasts. *PLoS ONE* 2009;4:e7475.
28. Gibbons MA, MacKinnon AC, Ramachandran P, Dhaliwal K, Duffin R, Phythian-Adams AT, van Rooijen N, Haslett C, Howie SE, Simpson AJ, et al. Ly6Chi monocytes direct alternatively activated profibrotic macrophage regulation of lung fibrosis. *Am J Respir Crit Care Med* 2011;184:569–581.
29. Murray LA, Rosada R, Moreira AP, Joshi A, Kramer MS, Hesson DP, Argentieri RL, Mathai S, Gulati M, Herzog EL, et al. Serum amyloid P therapeutically attenuates murine bleomycin-induced pulmonary fibrosis via its effects on macrophages. *PLoS ONE* 2010;5:e9683.
30. Auffray C, Sieweke MH, Geissmann F. Blood monocytes: development, heterogeneity, and relationship with dendritic cells. *Annu Rev Immunol* 2009;27:669–692.
31. Bedoret D, Wallemacq H, Marichal T, Desmet C, Quesada Calvo F, Henry E, Closset R, Dewals B, Thielen C, Gustin P, et al. Lung interstitial macrophages alter dendritic cell functions to prevent airway allergy in mice. *J Clin Invest* 2009;119:3723–3738.
32. Hume DA. Macrophages as APC and the dendritic cell myth. *J Immunol* 2008;181:5829–5835.
33. Geissmann F, Gordon S, Hume DA, Mowat AM, Randolph GJ. Unravelling mononuclear phagocyte heterogeneity. *Nat Rev Immunol* 2010;10:453–460.
34. Bantsimba-Malanda C, Marchal-Sommé J, Goven D, Freynet O, Michel L, Crestani B, Soler P. A role for dendritic cells in bleomycin-induced pulmonary fibrosis in mice? *Am J Respir Crit Care Med* 2010;182:385–395.
35. Marchal-Sommé J, Uzunhan Y, Marchand-Adam S, Kambouchner M, Valeyre D, Crestani B, Soler P. Dendritic cells accumulate in human fibrotic interstitial lung disease. *Am J Respir Crit Care Med* 2007;176:1007–1014.